Expanded View Figures

Figure EV1. NTRAS is essential for normal endothelial cell function.

A Illustration of the human *NTRAS* and *GAPDH* loci. Displayed are UCSC genome browser snapshots of ribosome profiling GWIPs-viz ribose tracks.
B Schematic representation of NTRAS transcript variants identified by RT–PCR and 5' RACE–PCR in HUVECs ($n = 1$).
C IGV screen shot showing NTRAS expression levels in HUVECs under normoxic (N) and hypoxic (H; 0.2% O_2 for 12 h or 24 h) conditions ($n = 2$ independent biological replicates).
D Digital PCR-based analysis of NTRAS copy numbers per μg of total RNA in HUVECs under normoxic (N) and hypoxic (H) conditions ($n = 3$ independent biological replicates).
E RT–qPCR-based analysis of VEGFA expression, controlling for hypoxia ($n = 4$ independent biological replicates).
F Subcellular localization of NTRAS in normoxic (N) and hypoxic (H) HUVECs, assayed by cellular fractionation and RT–qPCR ($n = 3$ independent biological replicates).
G RNAscope-based detection of NTRAS in HUVECs under normoxic and hypoxic conditions ($n = 1$). Binding sites of the probes are indicated.
H Validation of NTRAS silencing in HUVECs by RT–qPCR, comparing two different LNAs ($n = 4$ independent biological replicates).
I Cell cycle analysis in control and NTRAS-silenced HUVECs ($n = 3$ independent biological replicates).
J Representative images of *in vitro* sprouting comparing control and NTRAS-silenced HUVECs under basal conditions and VEGFA stimulation ($n = 3$–10 independent biological replicates). Scale bars are 50 μm.
K Illustration of the human and murine *NTRAS* loci (GRCh38.p13: RP11-354k1.1; GRCm38/mm10: 1700034H15).
L Validation of Ntras silencing in murine H5V cells by RT-qPCR ($n = 3$ independent biological replicates).
M RT–qPCR-based analysis of Ntras expression in hearts of control and Ntras-silenced mice ($n = 19$–23 mice per group).
N FTSC-based *in vivo* permeability assays, comparing heart homogenates from control and Ntras-silenced mice. Data normalized to organ and body weight ($n = 11$–12 mice per group). Experimental outline on the left.

Data information: In (D–F, H, I, L–N), data are represented as mean ± SEM. n.s.: non-significant, $*P < 0.05$, $**P < 0.01$, $***P < 0.001$. (D–F, H, I, L–N) two-tailed unpaired *t*-test.
Source data are available online for this figure.

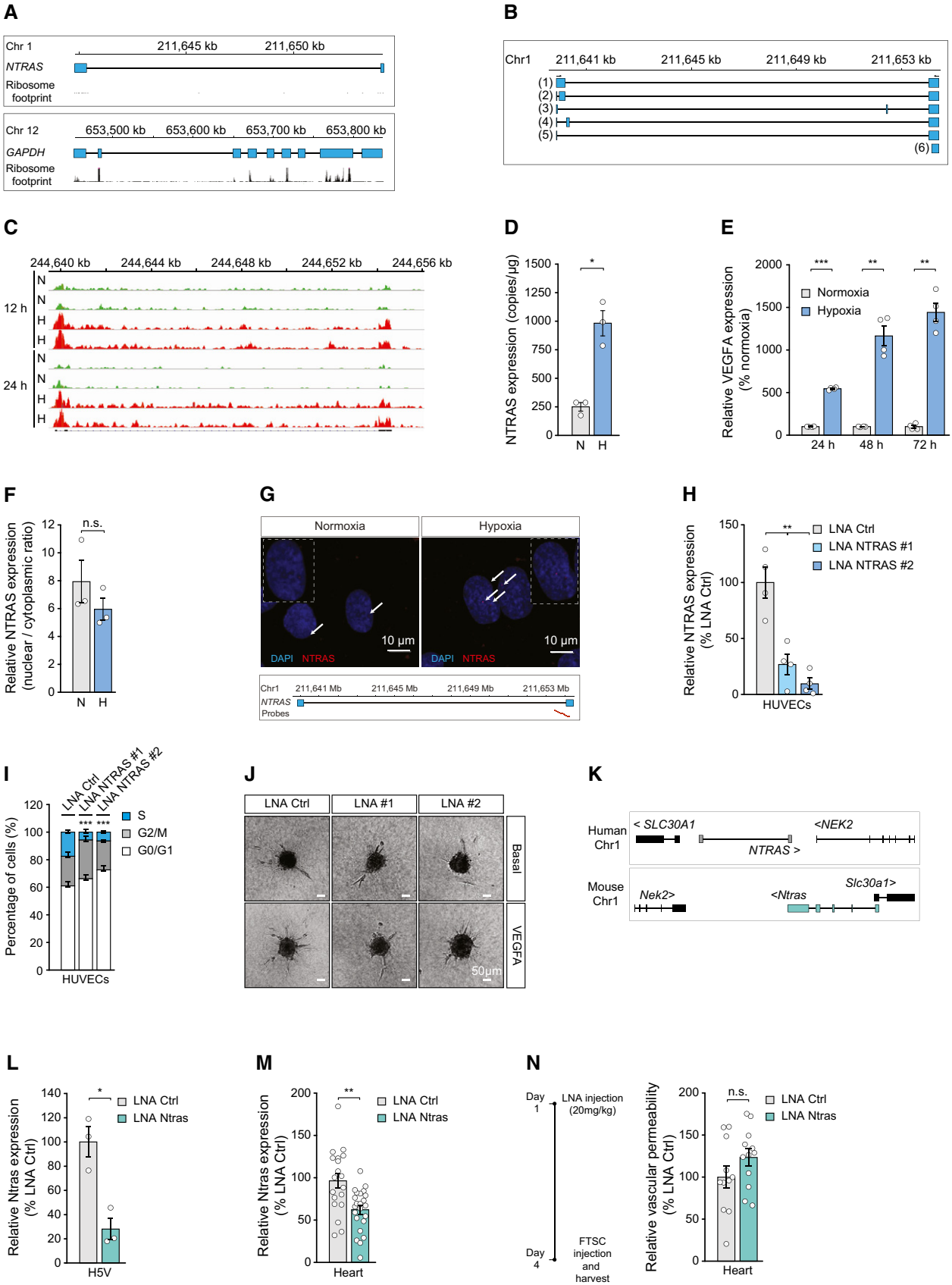
A
Chr 1
211,645 kb
211,650 kb
NTRAS
Ribosome footprint
Chr 12
653,500 kb
653,600 kb
653,700 kb
653,800 kb
GAPDH
Ribosome footprint
B
Chr1
211,641 kb
211,645 kb
211,649 kb
211,653 kb
(1)
(2)
(3)
(4)
(5)
(6)
C
244,640 kb
244,644 kb
244,648 kb
244,652 kb
244,656 kb
12 h
24 h
N
H
D
NTRAS expression (copies/µg)
N
H
E
Relative VEGFA expression (% normoxia)
Normoxia
Hypoxia
24 h
48 h
72 h
F
Relative NTRAS expression (nuclear / cytoplasmic ratio)
n.s.
N
H
G
Normoxia
Hypoxia
10 µm
DAPI NTRAS
Chr1
211,641 Mb
211,645 Mb
211,649 Mb
211,653 Mb
NTRAS
Probes
H
Relative NTRAS expression (% LNA Ctrl)
LNA Ctrl
LNA NTRAS #1
LNA NTRAS #2
HUVECs
I
LNA Ctrl
LNA NTRAS #1
LNA NTRAS #2
Percentage of cells (%)
S
G2/M
G0/G1
HUVECs
J
LNA Ctrl
LNA #1
LNA #2
Basal
VEGFA
50µm
K
Human Chr1
< SLC30A1
<NEK2
NTRAS >
Mouse Chr1
Nek2>
<Ntras
Slc30a1>
L
Relative Ntras expression (% LNA Ctrl)
LNA Ctrl
LNA Ntras
H5V
M
Relative Ntras expression (% LNA Ctrl)
LNA Ctrl
LNA Ntras
Heart
N
Day 1
LNA injection (20mg/kg)
Day 4
FTSC injection and harvest
Relative vascular permeability (% LNA Ctrl)
n.s.
LNA Ctrl
LNA Ntras
Heart

Figure EV1.

Figure EV2. NTRAS operates as splicing-regulatory lncRNA.

A Relative expression of NTRAS in HUVECs and HeLa cells, determined by RT–qPCR (n = 4 independent biological replicates).
B RT–qPCR-based identification of accessible regions within NTRAS using RNase H-mediated cleavage of RNA–DNA heteroduplexes (DNA antisense oligonucleotides AS1 to AS5) in HUVEC cell lysate (n = 1). The oligonucleotide used for probe design is highlighted in red.
C Scheme illustrating the affinity selection of endogenous NTRAS–protein complexes for RNA and protein analysis.
D Sucrose density gradient ultracentrifugation showing the distribution of NTRAS and hnRNPL (protein). The dashed box indicates the fractions with the greatest overlap of both factors (n = 1).
E Illustration of the human NTRAS locus. Displayed is *NTRAS* (GRCh38.p13; RP11-354k1.1) and RBPmap-predicted hnRNPL binding motifs, described elsewhere (Smith *et al*, 2013).
F Western blot-based validation of NTRAS–hnRNPL interaction following antisense affinity selection of NTRAS in nuclear extracts from normoxic and hypoxic HUVECs (n = 4 independent biological replicates).
G Expression of NTRAS in control and NTRAS-silenced HUVECs used for RNA sequencing (n = 4 independent biological replicates).
H hnRNPL mRNA levels in control and hnRNPL-silenced HUVECs used for RNA sequencing (n = 3 independent biological replicates).
I RT–PCR-based analysis of CD55 intron 7 retention following hnRNPL/NTRAS double knockdown in HUVECs (n = 4 independent biological replicates). Representative agarose gel on the right.
J rMATs-based analysis of alternative splicing events upon silencing of lncRNA lncflow2 in HUVECs (n = 4 independent biological replicates) ES: Exon skipping, MXE: Mutually exclusive exons, A5SS: Alternative 5' splice site, A3SS: Alternative 3' splice site, RI: Retained intron.
K Validation of hnRNPU silencing in HUVECs by RT–qPCR (n = 4 independent biological replicates).
L RT–PCR-based analysis of TJP1 exon 20 inclusion in hnRNPU-silenced HUVECs (n = 4 independent biological replicates).

Data information: In (A, F–I, K, L), data are represented as mean ± SEM. n.s.: non-significant, $^{**}P < 0.01$, $^{***}P < 0.001$. (A, F–H, K, and L) two-tailed unpaired t-test, and (I) one-way ANOVA.
Source data are available online for this figure.

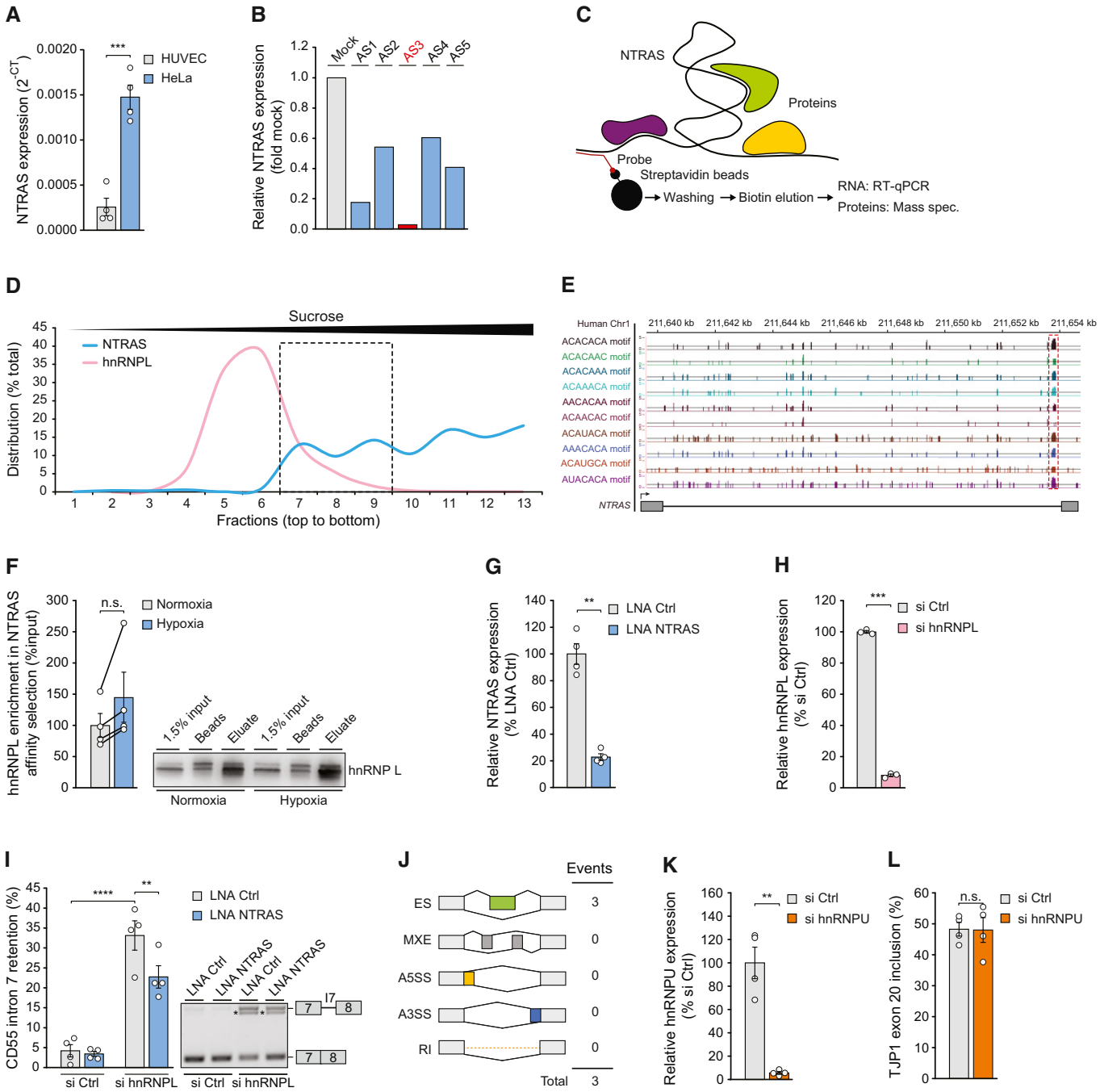
A
NTRAS expression (2-CT)
HUVEC
HeLa
B
Relative NTRAS expression (fold mock)
Mock
AS1
AS2
AS3
AS4
AS5
C
NTRAS
Proteins
Probe
Streptavidin beads
Washing
Biotin elution
RNA: RT-qPCR
Proteins: Mass spec.
D
Sucrose
NTRAS
hnRNPL
Distribution (% total)
Fractions (top to bottom)
E
Human Chr1
ACACACA motif
ACACAAC motif
ACACAAA motif
ACAAACA motif
AACACAA motif
ACAACAC motif
ACAUACA motif
AAACACA motif
ACAUGCA motif
AUACACA motif
NTRAS
F
hnRNPL enrichment in NTRAS affinity selection (%input)
n.s.
Normoxia
Hypoxia
1.5% input
Beads
Eluate
hnRNP L
G
Relative NTRAS expression (% LNA Ctrl)
LNA Ctrl
LNA NTRAS
H
Relative hnRNPL expression (% si Ctrl)
si Ctrl
si hnRNPL
I
CD55 intron 7 retention (%)
LNA Ctrl
LNA NTRAS
si Ctrl
si hnRNPL
J
Events
ES
MXE
A5SS
A3SS
RI
Total
K
Relative hnRNPU expression (% si Ctrl)
si Ctrl
si hnRNPU
L
TJP1 exon 20 inclusion (%)
n.s.
si Ctrl
si hnRNPU

Figure EV2.

Figure EV3. NTRAS controls TJP1 splicing and endothelial barrier function.

A RT–qPCR-based analysis of TJP1 mRNA expression in hnRNPL-silenced HUVECs ($n = 7$ independent biological replicates).
B Relative expression of BCL2, CASP3, CASP6, and CASP9 mRNA in hnRNPL-silenced HUVECs ($n = 2$ independent biological replicates).
C RT–qPCR-based analysis of TJP1 mRNA expression in NTRAS-silenced HUVECs ($n = 4$ independent biological replicates).
D RT–PCR-based analysis of Tjp1 exon 20 inclusion in control and Ntras-silenced murine CMT93 epithelial cells ($n = 3$ independent biological replicates).
E RT–qPCR-based validation of RNase H-mediated NTRAS degradation in HeLa nuclear extracts used for *in vitro* splicing ($n = 4$ independent biological replicates).
F RT–qPCR-based validation of NTRAS overexpression ($n = 4$ independent biological replicates).
G Co-precipitation of NTRAS in anti-hnRNPL RIPs, using nuclear lysates from control and NTRAS-overexpressing cells ($n = 4$ independent biological replicates).
H RT–PCR-based validation of NTRAS-CA_{16} motif overexpression ($n = 6$ independent biological replicates). Representative agarose gel on the right.
I Quantification of nuclear TJP1, comparing control and NTRAS-silenced HUVECs ($n = 4$ independent biological replicates). Representative micrographs are shown. Scale bars are 10 μm.
J Analysis of hnRNPL knockdown by western blot 72 h post-transfection of control or hnRNPL-targeting siRNAs ($n = 4$ independent biological replicates). Representative western blots on the right.
K *In vitro* permeability assays using FITC-dextran, comparing control and hnRNPL-silenced HUVECs ($n = 6$ independent biological replicates).
L *In vitro* permeability assays using FITC-dextran, comparing control and hnRNPU-silenced HUVECs ($n = 4$ independent biological replicates).
M *In vitro* permeability assays using FITC-dextran, comparing control SSO- and E20 SSO-transfected HUVECs ($n = 5$ independent biological replicates).

Data information: In (A, C–M) data are represented as mean ± SEM. n.s.: non-significant, *$P < 0.05$, **$P < 0.01$. (A–I) two-tailed unpaired *t*-test.
Source data are available online for this figure.

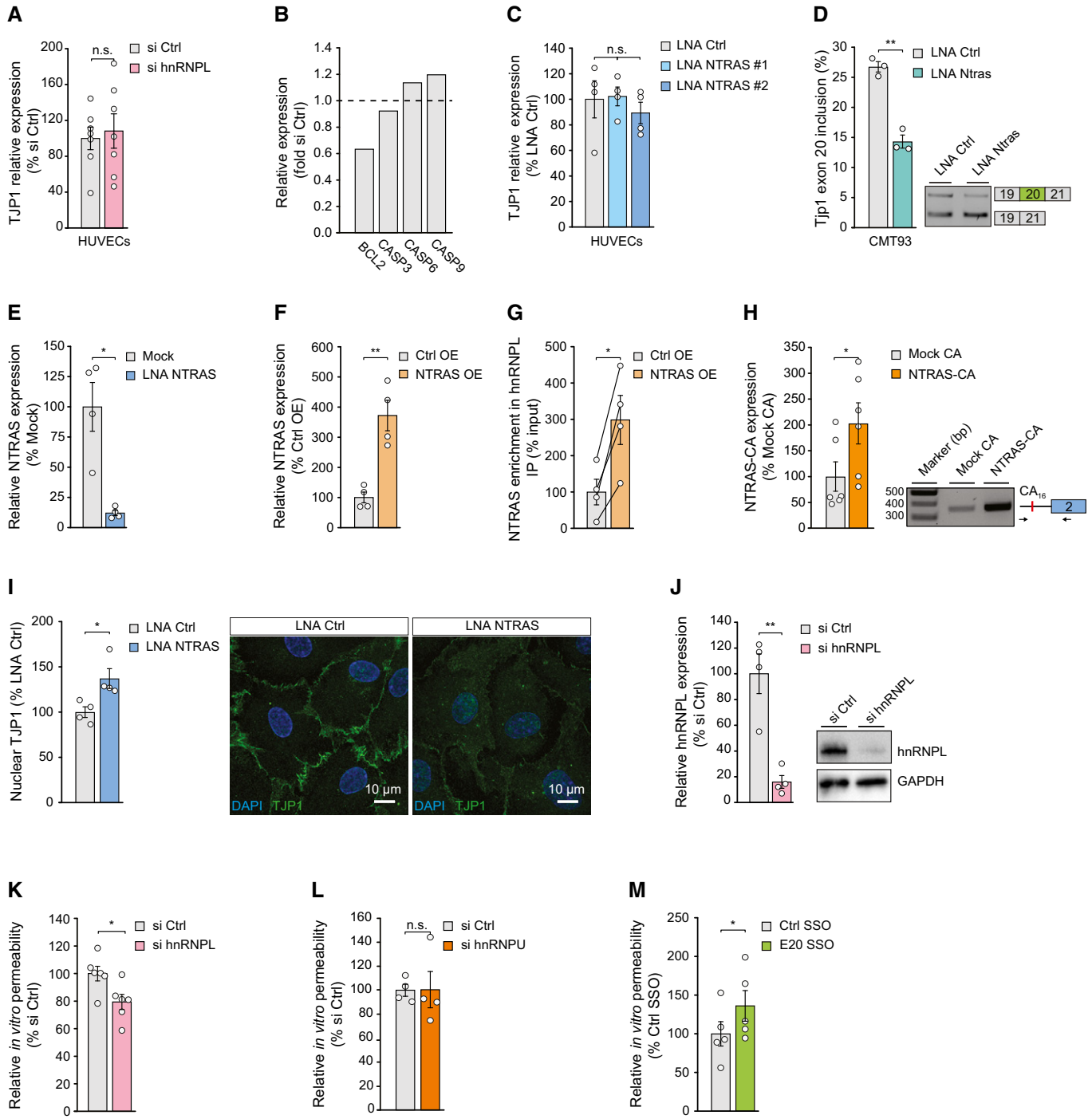
A
TJP1 relative expression (% si Ctrl)
n.s.
si Ctrl
si hnRNPL
HUVECs
B
Relative expression (fold si Ctrl)
BCL2
CASP3
CASP6
CASP9
C
TJP1 relative expression (% LNA Ctrl)
n.s.
LNA Ctrl
LNA NTRAS #1
LNA NTRAS #2
HUVECs
D
Tjp1 exon 20 inclusion (%)
LNA Ctrl
LNA Ntras
CMT93
19 20 21
19 21
E
Relative NTRAS expression (% Mock)
Mock
LNA NTRAS
F
Relative NTRAS expression (% Ctrl OE)
Ctrl OE
NTRAS OE
G
NTRAS enrichment in hnRNPL IP (% input)
Ctrl OE
NTRAS OE
H
NTRAS-CA expression (% Mock CA)
Mock CA
NTRAS-CA
Marker (bp)
Mock CA
NTRAS-CA
500
400
300
CA16
2
I
Nuclear TJP1 (% LNA Ctrl)
LNA Ctrl
LNA NTRAS
LNA Ctrl
LNA NTRAS
10 µm
DAPI TJP1
J
Relative hnRNPL expression (% si Ctrl)
si Ctrl
si hnRNPL
hnRNPL
GAPDH
K
Relative in vitro permeability (% si Ctrl)
si Ctrl
si hnRNPL
L
Relative in vitro permeability (% si Ctrl)
n.s.
si Ctrl
si hnRNPU
M
Relative in vitro permeability (% Ctrl SSO)
Ctrl SSO
E20 SSO

Figure EV3.

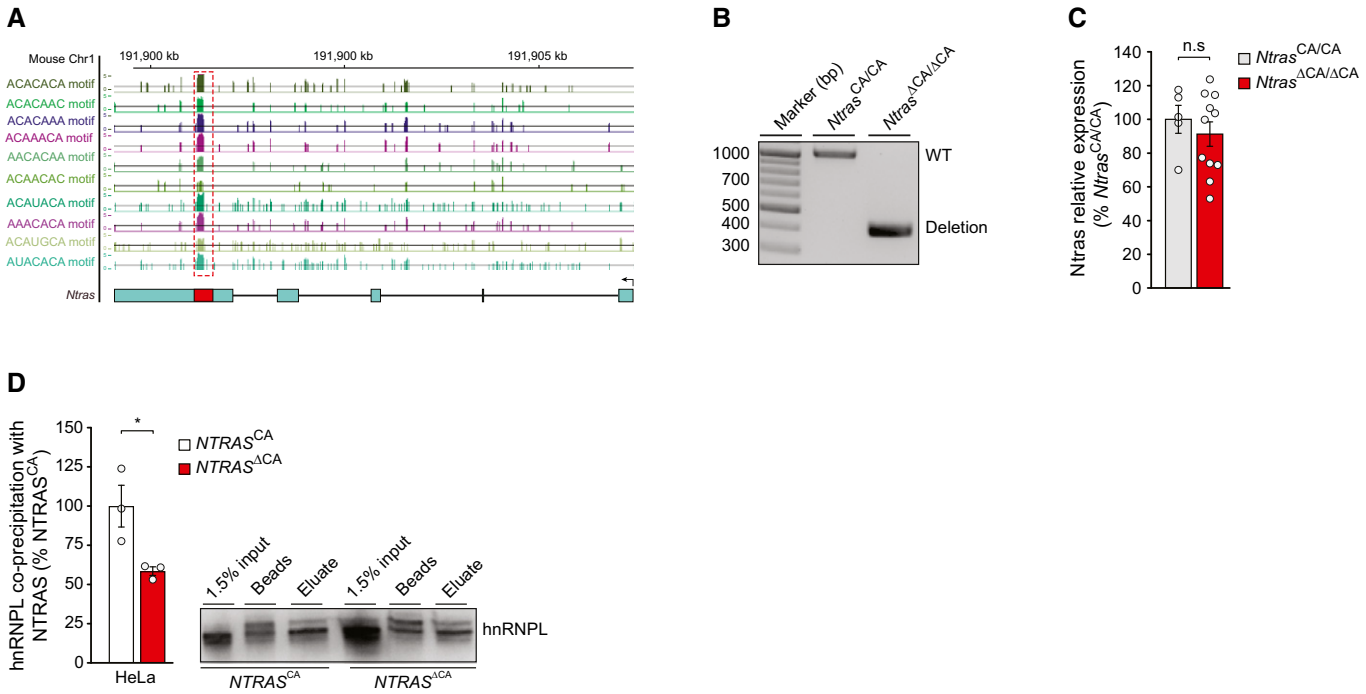

Figure EV4. Characterization of the Ntras CA-repeat *in vivo*.

A Illustration of the murine *Ntras* locus. Displayed is *Ntras* (GRCm38/mm10; 1700034H15) and RBPmap-predicted hnRNPL binding motifs, described elsewhere (Smith *et al*, 2013).

B Genotyping results confirming the genomic deletion of the hnRNPL binding motif in $Ntras^{\Delta CA/\Delta CA}$ mice.

C RT–qPCR-based analysis of Ntras expression in $Ntras^{CA/CA}$ and $Ntras^{\Delta CA/\Delta CA}$ mice (n = 5–11 mice per group).

D Western blot-based analysis of the NTRAS–hnRNPL interaction following antisense affinity selection of NTRAS in nuclear fractions from $NTRAS^{CA}$ controls and $NTRAS^{\Delta CA}$ HeLa cells (n = 3 independent biological replicates). Representative western blot on the right.

Data information: In (C, D), data are represented as mean ± SEM. n.s.: non-significant, $^*P < 0.05$. (C, D) two-tailed unpaired t-test.
Source data are available online for this figure.